THERMOREMANENT BEHAVIOR OF SMALL MULTIDOMAIN SYNTHETIC MAGNETITES

Vol. II

by

Gary D. Storrick

B.S.E., The University of Pittsburgh, 1977

M.S.E.E., The University of Pittsburgh, 1981

Submitted to the Graduate Faculty of

Arts and Sciences in partial fulfillment

of the requirements for the degree of

Doctor of Philosophy

University of Pittsburgh

1993

THERMOREMANENT BEHAVIOR OF SMALL MULTIDOMAIN SYNTHETIC MAGNETITES

Vol. I

by

Gary D. Storrick

B.S.E., The University of Pittsburgh, 1977

M.S.E.E., The University of Pittsburgh, 1981

Submitted to the Graduate Faculty of

Arts and Sciences in partial fulfillment

of the requirements for the degree of

Doctor of Philosophy

University of Pittsburgh

1993

UNIVERSITY OF PITTSBURGH

FACULTY OF ARTS AND SCIENCES

This dissertation was presented

by

Gary D. Storrick

It was defended on

July 28, 1993

and approved by

Jean Blachere

William Harbert

Edward Lidiak

Walter Pilant

William Soffa

Committee Chairperson Victor A. Schmidt

THERMOREMANENT BEHAVIOR OF SMALL MULTIDOMAIN SYNTHETIC MAGNETITES

Gary D. Storrick, Ph. D.

University of Pittsburgh, 1993

This study investigates the details of how Néel-type theories of multidomain TRM are violated for high quality synthetic magnetites produced by the glass-ceramic method of Worm and Markert [1987]. The glass-ceramic method provides a simple means of preparing nearly uniformly-sized, dispersed, almost chemically pure, and relatively unstressed magnetite crystals that are well-suited for this work.

Six samples were selected for detailed study. SEM observations showed well-formed magnetite crystals with diameters ranging from 0.8 to 5.8 μm, well within the multidomain range yet small enough to display pseudo-single-domain behavior. The samples were heated to slightly above the magnetite Curie temperature, then allowed to cool in an applied magnetic field. Fourteen cases per sample were run using fields ranging from 10 μT to 30 mT. The resulting TRM curves show the M_{TRM} B^{1} dependency expected at low fields, with a smooth transition towards saturation in the higher fields. Saturation was not reached, even in the 30 mT cases. The distinct thermal-activation blocking (M_{TRM} B^{1}), Néel blocking (M_{TRM} $B^{1/2}$), and saturation regions discussed by Schmidt [1973, 1975] are not readily apparent.

In each case, the sample was sequentially demagnetized using alternating fields ranging from 5 mT to 140 mT. The demagnetization curves for most samples show a shift in the coercivity spectrum of the grains contributing to

the TRM, with an increase in the importance of the low-coercivity grains as the applied field is increased. This contradicts the behavior predicted when the Schmidt-Néel theory is applied to an assemblage of grains. The 5.8 μm sample showed anomalous behavior, which is attributed to the relatively large variation in grain size within the sample.

Theory predicts a shift in blocking temperature to lower temperatures as the applied field is increased. This can be observed through the field-dependence of partial TRM (PTRM), provided the high-temperature isothermal-remanence (IRM) is taken into account as a correction. A series of PTRM and high-temperature IRM acquisition runs demonstrated that the predicted shifts occur, and that Thellier's Law of Additivity of PTRMs was satisfied.

ACKNOWLEDGEMENTS

This project could not have been completed without the assistance of several individuals. Dr. Horst Worm showed me how to make samples using the glass-ceramic technique. Dr. Michael Bickerman encapsulated the samples for me, and provided access to his glass-blowing equipment as needed. Jennifer Spear operated the x-ray diffractometer, Tim Klemmer taught me how to operate the vibrating sample magnetometer, and Dr. Jean Blachere ran the scanning electron microscope. The National Science Foundation provided funding for this work.

The members of the Doctoral Committee each provided many helpful suggestions.

Finally, I would like to thank Dr. Victor Schmidt for his patient encouragement over the past several years.

TABLE OF CONTENTS

LIST OF FIGURES

LIST OF TABLES

LIST OF SYMBOLS

Symbol	Units	Description
A	kg m^{-1} A^{-1} s^{-2}	Constant in §3.2
B	kg m^{-1} s^{-2}	Constant in §3.2
C	s^{-1}	Frequency factor
D	kg m^{-3} s^{-2}	Constant in §3.2
D	-	Demagnetizing factor
d	m	Effective grain diameter
E	J = kg m^2 s^{-2}	Energy
F	-	Constant in §3.2.2
H	A m^{-1}	Magnetic field strength
I	A	Current
J	T = kg m^2 s^{-2}	Magnetic polarization (<u>not</u> current density)
K	(as required)	Constant, as required, see text
k	J K^{-1}=kg m^2 K^{-1} s^{-2}	Boltzmann constant, 1.38×10^{-23} J K^{-1}
L	m	Grain length in §3.2

Symbol	Units	Description
L(x)	-	Langevin function, $L(x) = \coth(x) - \frac{1}{x}$
m(T)	-	Reduced magnetization $m(T) = \frac{M_s(T)}{M_s(0)}$
m	A m^2	Magnetic dipole moment
M	A m^{-1}	Magnetization
M_s	A m^{-1}	Saturation magnetization
p	-	Exponent in §3.2
q	(as required)	Constant, as required, see text
T	K	Temperature
T_c	K	Curie temperature
T_b	K	Blocking temperature
v	m^3	Grain volume
x	m	Wall position in §3.2
Z	-	Partition function
Δh	m	Manometer height difference
λ	m	Defect spacing
τ	s^{-1}	Time constant
$\tau(0,\pi)$	s^{-1}	Alignment time constant in §3.1
$\tau(\pi,0)$	s^{-1}	Misalignment time constant in §3.1

Symbol	Units	Description
μ_0	$H\ m^{-1} = kg\ m\ A^{-2}\ s^{-2}$	Permeability of free space, $4\pi \times 10^{-7}$ $H\ m^{-1}$
ω	$m^3\ s^{-1}$	Flow
a	(subscript)	Ambient (room) temperature
b	(subscript)	Blocking temperature
c	(subscript)	Curie temperature
s	(subscript)	Saturation
THB	(subscript)	Thermal-activation blocking
ub	(subscript)	Unblocking temperature

1.0 INTRODUCTION

Paleomagnetism occupies a unique position among geophysical techniques due to the ability of certain rocks to preserve a record of the local Earth's magnetic field throughout geologic times. Initially even first-order interpretations of the paleomagnetic record were significant, as evidenced by the substantial support paleomagnetism provided for plate tectonic theory. More recently, paleomagnetic studies have pushed toward obtaining higher temporal and spatial resolution. The success of these efforts is critically dependent on an understanding of the remanent mechanisms operating in rocks, and in particular on the mechanism of thermoremanent magnetization (TRM), which is the principal source of remanence in igneous rocks and a likely source for the original magnetization in detrital grains in sedimentary rocks.

A rigorous theory of TRM based on first principles appears to be presently unattainable. The accepted quantum mechanical model for ferromagnetism involves a primitive cubic array of atoms with an electron spin of $s=\pm 1/2$ associated with each lattice site [Pathria, 1972]. Although the mathematical model [Heisenberg, 1928] is widely known, solutions have only been obtained for the Ising approximation in the one-dimensional [Ising, 1925] and the field free two-dimensional [Onsager, 1944] cases. Topological considerations [Kac and Ward, 1952] argue against obtaining three-dimensional solutions to the Ising problem by similar techniques. Considering physicists' failure to solve the Ising model despite six decades of trying, there is little reason to expect a

rigorous description of TRM in real materials at any time in the immediate future.

Practical TRM theories have taken a less rigorous approach. These theories can be divided into two categories. The classical approach involves developing simple analytical models of idealized magnetic particles. Néel's two classic papers on single-domain (SD) [Néel 1949] and multidomain (MD) [Néel, 1955] magnetic grains form the starting point for most of these studies. More recent studies have invoked an intermediate "pseudo-single-domain" (PSD) grain behavior to explain the continuity of experimentally measured parameters across the predicted SD-MD boundary, but to date these efforts have been inconclusive. Some of the competing explanations for pseudo-single domain mechanisms are:

1. Barkhausen discreteness of domain wall motions [Stacey, 1962]
2. surface domains [Stacey and Banerjee, 1974; Banerjee, 1977; Moskowitz and Banerjee, 1979]
3. domain wall moments with SD-like properties [Dunlop, 1977]
4. moments pinned by stress fields of dislocations [Verhoogen, 1959; Ozima and Ozima, 1965]
5. expected MD-size grains in metastable SD or SD-like states [Halgedahl and Fuller, 1980, 1983]
6. intrinsic SD-like properties of small MD grains [Fuller, 1984]

The TRM mechanism for SD grains is fairly well understood in terms of Néel's SD model, though some discrepancies remain. The agreement between experiment and the available Néel domain wall motion theories for MD grains is much less satisfactory, particularly for the small MD grains which in practice dominate the TRM of so many rocks. To date, explanations of the discrepancies have been less than satisfactory. Previous work indicates that Néel-type models of TRM are qualitatively useful but quantitatively

inaccurate. This study investigates the details of how Néel-type theories of MD TRM are violated for high quality synthetic magnetites produced by the glass-ceramic method of Worm and Markert [1987b].

Numerous studies have examined magnetic properties of titanomagnetite particles in the SD, PSD, and small MD size range. Most of these studies were hampered by the difficulties involved in preparing uniform samples for study. Recently a glass-ceramic technique has been developed which provides well-dispersed titanomagnetite particles in a silicate matrix [Worm and Markert, 1987b]. Worm [1986] reports he has used samples prepared in this manner to verify Néel's SD theory. This study produced samples by this glass-ceramic method, then proceeded to magnetically characterize the samples with the intent of carefully understanding the details of how the MD Néel models are violated, thus providing guidance for modifying the Néel-type MD models.

Néel-type MD theories are based on domain wall motion only, and usually on that of only a single wall. They omit the demonstrable influence of domain wall nucleation [Boyd et al., 1984]. Theories incorporating domain wall nucleation have been proposed [Moon, 1985], but currently are formulated in a micromagnetic approach requiring extensive numerical calculation. A very simple demonstration of the inadequacy of Néel-type theories is that they predict that for MD particles TRM acquired in a strong field is more stable with respect to AF demagnetization than TRM acquired by the same sample in a weak field [Schmidt, 1976], whereas the converse is experimentally observed in small MD particles. This has been partially, but not fully, resolved by considering the interaction effects between walls when more than one wall is present [Schmidt, 1975], and by taking into account demagnetizing field effects [Bailey and Dunlop, 1983].

There is a need for a simpler model which incorporates domain wall nucleation without requiring the extensive calculations involved in the micromagnetic approach. One immediate suggestion is incorporating a potential barrier against nucleation into a Néel-type model such as Schmidt's

[1973], while introducing assemblages of different grains that may or may not contain walls. Another approach would allow multiple interacting walls in one grain, with nucleation effects determining the number. Clearly, experimental results are needed as a guide in the construction of such models.

It is generally understood that synthetic materials can provide simpler systems for theoretical modeling than natural titanomagnetites. Natural titanomagnetites are often both nonstoichiometric and impure. Most natural titanomagnetites do not lie upon the ulvöspinel-magnetite join, but are slightly oxidized towards the ilmenite-magnetite join [Nagata, 1961]. Al^{3+}, Mg^{2+}, Mn^{2+} and other cations are known to substitute for Fe^{3+} or Fe^{2+}. Although numerous authors have investigated the effects of oxidation [Readman and O'Reilly, 1970; Ozima and Sakamoto, 1971; Rahman and Parry, 1978] and cation substitution [Özdemir and O'Reilly, 1978; Richards et al., 1973], natural systems still provide too many complications for convenient theoretical treatment and too much variability for comparison of results with theory. Synthetic materials can provide samples with fewer variations in composition and grain size distribution, and hence are more amenable to theoretical treatment.

Synthetic samples have been prepared by several methods:

1. Hydrothermal method [Lindsley, 1962; Pucher, 1969]
2. Grinding sintered titanomagnetites and dispersing sieved fragments in a nonmagnetic matrix [Day, 1977; Clauter, 1979]
3. Aqueous precipitation [Dunlop, 1973; Clauter, 1979]
4. Bridgman method [Syono, 1965; Hauptman and Stephenson, 1968]
5. Flux method [Hauptman et al., 1973]
6. Glass-ceramic method [Worm and Markert, 1987a]

The study samples were produced by the glass-ceramic method. The synthesis procedure consists of melting a mixture of oxides/carbonates of Ca, K, Na, Si, Fe and Ti under a controlled reducing atmosphere, then quenching the melt to a glass. Two heat treatment steps under controlled atmosphere allow nucleation and growth of titanomagnetite crystals respectively, and are followed by a final quench.

The glass-ceramic method has several advantages. First, it is amenable to crystal growth in a controlled atmosphere, and hence stoichiometry can be controlled. The resulting titanomagnetite crystals are dispersed throughout a magnetically inert matrix, minimizing the effects of intergrain interactions. The matrix acts as a barrier to oxygen, thus protecting the titanomagnetite crystals from chemical alteration. Crystals are easily produced in the grain sizes corresponding to the SD through MD transition. The heat treatment process allows one to maintain relatively close control over the size distribution for a wide range of crystal sizes. Stresses in the resulting crystals are less than those introduced by methods involving sample grinding. These advantages are illustrated by the first published results using the glass-ceramic titanomagnetites, where SD and MD hysteresis results disagree with previous studies, yet were found to be in better agreement with theory [Worm and Markert, 1987a].

Initially I proposed working with various-sized grains of a single titanomagnetite composition. I originally planned to use a moderately high-titanium titanomagnetite (approximately $Fe_{2.5}Ti_{0.5}O_4$) with a fairly low Curie temperature of ~ 200 °C, thus reducing the probability of chemical alteration during the TRM experiments. Comments received during the NSF review of the research grant proposal, conversations with Dr. Worm, and the possibility of magnetite/ulvöspinel exsolution complicating the results convinced me to work with magnetite instead.

The heating and cooling for the TRM studies was performed in the TRM furnace built and described by Clauter [1979]. Although the TRM furnace is equipped for maintaining a controlled atmosphere and this feature was used

in this study, the process requires careful attention and is somewhat of a nuisance. Since I did not need to exceed the Curie temperature by much in these experiments, I could not rely on using equilibrium atmospheres to prevent sample oxidation since equilibration is unlikely to occur at such low temperatures. I tried to eliminating chemical change in the samples during the magnetic experiments by isolating the samples from the atmosphere. The method I chose was to seal the samples in evacuated quartz tubes to minimize the probability of chemical alteration and to provide self-buffering. The samples were then thermally cycled from room temperature to beyond their Curie temperature until their magnetic properties stabilized. The sample preparation furnace was used because the electronic temperature controller was easily programmed to automate the desired temperature cycling process.

An original fragment of each sample was preserved for comparison to determine the extent of chemical alteration during the thermal cycling process, and the characterization process was repeated after the magnetic experiments were completed to determine the extent and nature of any changes. The synthesized magnetites were characterized by x-ray diffraction, SEM, and electron microprobe. Magnetic hysteresis properties were measured on Material Engineering's vibrating sample magnetometer equipped with a temperature controlled sample holder. Isothermal remanent magnetization (IRM) curves were measured using the Paleomagnetism Laboratory's spinner magnetometer, while TRM, partial TRM (PTRM), and additional IRM properties were measured in the Paleomagnetism Laboratory's cryogenic magnetometer.

2.0 STATEMENT OF PROBLEM

Two classic experiments were performed. The first was to measure TRM acquisition versus the strength of an externally applied field. The second was to measure the shift in blocking temperature versus applied field by making a series of PTRM measurements. The first reaction of the reader may well be that this appears to be a rather old-fashioned approach, and it is, at least in its initial stages. The problem with the newer theoretical models that are being used is that they have tended to a micromagnetic approach. While obviously desirable, they have the disadvantage of requiring detailed knowledge of grain size and shape. Also, at present they are not easily generalized to bulk properties, which is what one must work with in the laboratory.

The strength of the Néel models has always been their simplicity. They clearly err in the direction of being generalizations that are too broad, and the MD model in particular may be faulted as missing the mark entirely if, for instance, domain nucleation is a more important process than domain wall displacement, or if moments intrinsic to the domain structure such as wall moments are of overriding importance. What one needs are experimental results that show just which predictions of the old Néel models are correct and which are not, for the new class of glass-ceramic synthetic titanomagnetites.

In two early papers, Schmidt [1973, 1976] pointed out the critical role that the variation of blocking temperature plays in both the SD and MD Néel models. It is evident that the broad behavior demonstrated in the 1976 paper

of $T_B(H)$ must in fact be operational. Only if $T_B(H)$ decreases with increasing field H can one obtain the observed and universal rule that TRM approaches IRM in all its properties as H becomes large compared to microscopic coercivity. From this, it is easy to show that the MD Néel model predicts that unblocking should take place at a lower temperature than blocking. The formal argument is summarized in Section 3.2.

Worm et al.'s [1988] recent work shows that the synthetic glass-ceramic samples support the earlier work reported by Bolshakov and Shcherbakov [1979], which was carried out on traditionally prepared samples, in which a partial TRM acquired in a moderate temperature range is not demagnetized in zero field until a much higher temperature. This appears to fly in the face of the $T_B(H)$ behavior just discussed, but may reflect instead complications that are not present in the basic Néel models, such as interactions between domain walls and nucleation effects.

Thus, one of the highest priorities was to repeat some of the experiments of Clauter [Clauter, 1979; Clauter and Schmidt, 1981] in which it was shown that the partial TRM spectrum did in fact shift to lower temperatures as the field H increases. Note that this is not the same experiment done by Worm et al. [1988], which tests the relation between blocking and unblocking temperatures, but directly tests the $T_B(H)$ dependence. If Clauter's results are borne out in the synthetic samples, then there would be a basis for extending the original Néel MD model, based on the $T_B(H)$ dependence, but searching for additional terms that would reverse the blocking-unblocking relation.

First, I made measurements of TRM acquisition versus applied field. Previous workers [Dunlop, 1975; Day, 1977] have reported power-law dependencies in TRM(H) acquisition curves, while Clauter [1979] failed to find such a dependence for carefully-sized synthetic samples. A problem in interpreting these results is that grain size and shape variation within each bulk sample tends to smear out the breaks between the three segments of the acquisition curve predicted by the Néel MD theory (low-field linear during thermal fluctuation blocking, approach to saturation in which the effect of the

demagnetizing field is dominant, and finally saturation). The relatively uniform sizes and shapes of the dispersed magnetite grains produced by the glass-ceramic method yield much clearer and more reliable results, perhaps at last settling in the negative a very old question as to whether these power-law segments are in fact real.

Second, I investigated the variation of the blocking temperatures versus applied field, along the lines used by Clauter and Schmidt [1981]. This was accomplished through a series of PTRM acquisitions. Worm et al. [1988] performed some thermal demagnetization of PTRMs as part of a viscous magnetization study, but their experiments were limited to low field strengths (0.05-0.5 mT) and included only a single PTRM temperature interval. This work included more complete PTRM study and provides valuable data on the effect of applied field on blocking and unblocking temperatures, and hence provides valuable insight on the TRM mechanism in small MD grains. To this end, the PTRM acquisition spectra were supplemented by alternating-field demagnetization curves for individual PTRMs as well as for total TRMs.

In each case past work has indicated violation of the quantitative predictions of Néel-type models; by carefully measuring these deviations I hoped to gain some insight into the mechanisms not considered in the Néel models. These are summarized in Sections 7 and 8.

3.0 REVIEW OF ROCK MAGNETIC THEORIES

3.1 SD theories

3.1.1 The Néel SD model

The TRM mechanism for small particles must treat the particles as a single domain, for the simple reason that there is insufficient room in a small particle for a domain wall to form. More precisely, formation of a domain wall in small particles carries an energy penalty that can not be offset by a corresponding reduction in magnetostatic energy. A domain wall can only form in grains that are large enough for the change in magnetostatic energy (which is roughly proportional to grain volume) to exceed the increase in exchange energy associated with wall motion (roughly proportional to grain diameter). For this reason, theories of SD behavior have been developed. These theories all consider uniformly magnetized grains, and attribute changes in bulk magnetization to changes in the distribution of the magnetization directions of the individual grains

Néel [1955] proposed a theory of SD TRM that explains the observed linear dependence of TRM on the applied field H for low fields. Noting that an explanation based on the coercive force H_c approaching zero as temperature approaches the Curie temperature T_c fails to account for any field dependence, he introduced a model where thermal agitation acted to demagnetize a grain if the temperature was high enough. Specifically, the remanent moment $m(t)$ of an assemblage of identical grains will decay to zero exponentially with time t as

$$(t) = \quad {}_0 e^{-\frac{t}{\tau}}. \tag{3.1.1-1}$$

The time constant τ is given by

$$\tau = C^{-1} e^{\left[\frac{v\mu_0 M_s(T) H_c(T)}{2kT}\right]}, \tag{3.1.1-2}$$

where C is a constant on the order of 10^{10} s^{-1} whose form does not concern us here, v is the grain volume, $H_c(T)$ is the microscopic coercive force at temperature T, $M_S(T)$ is the saturation magnetization, and k is Boltzmann's constant. In an applied field H, Néel derived two relaxation times $\tau(0,\pi)$ and $\tau(\pi,0)$ for alignment and misalignment, respectively. These were given by

$$\tau(0,\pi) = C^{-1}\left(1 + \frac{H}{H_c(T)}\right)\left(1 - \frac{H^2}{H_c^2(T)}\right)^{\frac{1}{2}} e^{\left[\frac{v\mu_0 M_s(T)(H_c(T)+H)^2}{2H_c(T)kT}\right]} \tag{3.1.1-3}$$

and

$$\tau(\pi,0) = C^{-1}\left(1 - \frac{H}{H_c(T)}\right)\left(1 - \frac{H^2}{H_c^2(T)}\right)^{\frac{1}{2}} e^{\left[\frac{v\mu_0 M_s(T)(H_c(T)-H)^2}{2H_c(T)kT}\right]}, \tag{3.1.1-4}$$

respectively, and the effective relaxation time constant for the assemblage is given by

$$\frac{1}{\tau} = \frac{1}{\tau(0,\pi)} + \frac{1}{\tau(\pi,0)}. \tag{3.1.1-5}$$

The time constant's exponential dependence on temperature shows that there is a narrow temperature range over which the time constant changes from a large time at low temperature to a small time at high temperature. This motivates defining a blocking temperature T_b, and making the simplifying assumption that equilibration is reached instantaneously for $T > T_b$, while no relaxation occurs for $T < T_b$. In practice, the blocking temperature is defined by first selecting a blocking time τ_b corresponding to

the time scale for the experiment in question. The blocking temperature is then defined as the temperature at which $\tau = \tau_b$.

Perhaps the simplest model of the field-dependence of TRM assumes an assemblage of identical, noninteracting SD particles where each grain has a uniaxial magnetic anisotropy aligned parallel to the applied field. The partition function Z for such an assemblage in equilibrium is

$$Z = e^{\left(\frac{v\mu_0 M_s(T)H}{kT}\right)} + e^{\left(-\frac{v\mu_0 M_s(T)H}{kT}\right)}, \tag{3.1.1-6}$$

and the average magnetization when $T > T_b$ is given by

$$M(T) = \left(\frac{1}{v\mu_0}\right) kT \frac{\partial \ln(Z)}{\partial H} = M_s(T)\tanh\left(\frac{v\mu_0 M_s(T)H}{kT}\right). \tag{3.1.1-7}$$

Below the blocking temperature, the relaxation time of the assemblage is long compared to the experiment, so the magnetization is assumed to be fixed at a value determined by past history. The TRM process fixes the past history in a manner that the TRM can be easily calculated. After heating to the Curie temperature and cooling in a weak field H, the TRM of an assemblage of such grains below the blocking temperature is given by

$$M_{TRM}(T) = M(T_b)\frac{M_s(T)}{M_s(T_b)} = M_s(T)\tanh\left(\frac{v\mu_0 M_b(T_b)H}{kT_b}\right), \tag{3.1.1-8}$$

where $M_b \equiv M(T_b)$ and $H(T_b)$ is written explicitly to emphasize that the TRM is caused by the applied field at the time the grains cool below their blocking temperature.

The preceding discussion neglects the blocking temperature's dependence on the applied field. In Néel's formulation, the variation in thermal relaxation time with applied field makes the blocking temperature a function of the applied field. Schmidt [1976] combined equations (3.1.1-3), (3.1.1-4), and (3.1.1-5) for $T = T_b$ to give the following implicit formula for the blocking temperature:

$$M_b = \left(\frac{2H_{C_b}kT_b}{v\mu_0\left(H_{C_b}-H\right)^2}\right)\ln\left(\tau_b C\left(1-\frac{H^2}{H_{C_b}^2}\right)^{\frac{1}{2}}\left(1-\frac{H}{H_{C_b}}\right)+\left(1+\frac{H}{H_{C_b}}\right)e^{-\frac{2v\mu_0 M_b H}{kT_b}}\right). \quad (3.1.1\text{-}9)$$

This can be solved numerically for $M_b(T)$ once the temperature dependence of H_c is known. Schmidt recommends using

$$H_{C_b} = KM_b^{q-1}, \quad (3.1.1\text{-}10)$$

where K is a constant in the range of 0 to 1 and q can be varied in the range of 2 to 10 to accommodate various types of magnetic anisotropy (e.g., shape, crystalline, and magnetostrictive). He recommends using a value close to 2 for the common case when shape anisotropy dominates. Substituting (3.1.1-10) into (3.1.1-9) allows one to numerically determine M_b and T_b, which are then substituted into (3.1.1-8) to give the TRM field dependence for SD grains.

Luce [1980] questioned the assumptions leading to (3.1.1-7). He preferred using the Langevin function as a starting point, rather than the hyperbolic tangent. The Langevin function $L(x) \equiv \coth(x) - x^{-1}$ arises when one considers a Boltzmann assemblage of uniaxial particles that may move and take any orientation with respect to the field. The partition function for this condition is given by

$$Z = \int_0^{\pi} e^{\frac{v\mu_0 M_s(T) H\cos(\theta)}{kT}}\sin(\theta)d\theta, \quad (3.1.1\text{-}11)$$

the corresponding average magnetization above the blocking temperature is given by

$$M(T) = \left(\frac{1}{v\mu_0}\right)kT\frac{\partial\ln(Z)}{\partial H} = M_s(T)\,L\left(\frac{v\mu_0 M_s(T)H}{kT}\right), \quad (3.1.1\text{-}12)$$

and the TRM is given by

$$M_{TRM}(T) = M(T_b)\frac{M_s(T)}{M_s(T_b)} = M_s(T)L\left(\frac{\nu\mu_0 M_b H(T_b)}{kT_b}\right). \quad (3.1.1\text{-}13)$$

As before, M_b is given by (3.1.1-9) and T_b is calculated using (3.1.1-3), (3.1.1-4), and (3.1.1-5). Luce's reasons for preferring this model will be given after the next model is discussed.

Stacey and Banerjee [1976] introduced a model that accounted for a randomly-oriented distribution of identical noninteracting particles, each of which possessed a uniaxial magnetic anisotropy. The partition function for a particle aligned with the easy direction at angle θ to the applied field is given by

$$Z = e^{\left[\frac{\nu\mu_0 M_s(T)H\cos(\theta)}{kT}\right]} + e^{\left[-\frac{\nu\mu_0 M_s(T)H\cos(\theta)}{kT}\right]}. \quad (3.1.1\text{-}14)$$

For these grains, the corresponding average magnetization above the blocking temperature is given by

$$M(T) = \left(\frac{1}{\nu\mu_0}\right)kT\frac{\partial \ln(Z)}{\partial H} = M_s(T)\cos(\theta)\tanh\left(\frac{\nu\mu_0 M_s(T)H\cos(\theta)}{kT}\right). \quad (3.1.1\text{-}15)$$

Integrating over all orientations gives the average magnetization for all grains. The corresponding TRM is given by

$$M_{TRM}(T) = M(T_b)\frac{M_s(T)}{M_s(T_b)} = M_s(T)\int_0^{\pi/2}\cos(\theta)\tanh\left(\frac{\nu\mu_0 M_b H(T_b)\cos(\theta)}{kT_b}\right)\sin(\theta)d\theta. \quad (3.1.1\text{-}16)$$

As before, M_b is given by (3.1.1-9) and T_b is calculated using (3.1.1-3), (3.1.1-4), and (3.1.1-5).

Luce extended Stacey and Banerjee's approach by considering a cubic magnetite crystal with eight easy directions of magnetization. The resulting field-dependence was obtained numerically, and found to be closer to the

Langevin model than either the hyperbolic tangent model or the Stacey-Banerjee model. For this reason, he preferred the Langevin model.

Each of these models shares the following characteristics:

1. TRM is a continuous, smooth, monotonic, increasing function of the applied field.

2. TRM is a linear function of the applied field at low fields, and saturates at high fields.

These characteristics will be compared to those for MD particles in Section 3.2.1.

3.1.2 Unblocking in the Néel domain-reversal mechanism

Schmidt [1976] examined (3.1.1-9) and (3.1.1-10) for the case with $q = 2$. By neglecting the variation in the argument of the logarithm, he was able to show that $H_{C_b} > H$ and T_b decreases with increasing H. For unblocking, as measured in the laboratory with $H = 0$, we can define an unblocking temperature T_{ub}. The unblocking temperature is given by the same equation as the blocking temperature (with $H = 0$), and so immediately we see that $T_{ub} < T_b$, and the difference $T_b - T_{ub}$ increases as H increases. A somewhat different result will be obtained for MD grains in Section 3.2.2.

3.2 MD theories

3.2.1 The Néel-Schmidt MD model

Schmidt [1972] constructed a model of MD TRM from first principles. His model is physically equivalent to Néel's [1955] MD model. Néel based his model on the temperature dependence of a secondary characteristic, the microscopic coercive force. Schmidt's model is based on the interaction of a single domain wall with the applied field, the demagnetizing field of the

grain, and a periodic array of pinning sites within the grain. The model assumes a grain of width L with a single 180° wall of area A offset a distance x from the grain center. The external field is applied parallel to the axis of domain magnetization. Defining the reduced magnetization $m(T) = \frac{M_s(T)}{M_s(0)}$ for convenience, Schmidt gives the energy relation

$$\frac{E}{v} = -\ Hmx + \ m^2x^2 - \ m^p \cos\left(\frac{2\pi x}{\lambda}\right). \qquad (3.2.1\text{-}1)$$

The first term describes the magnetostatic interaction between the grain and applied field, where $= 2\mu_0 M_s(0)/L$. (This differs from Schmidt's usage by a factor of μ_0). The second term represents the self-energy $\mu_0 D M^2 v/2$ of the grain demagnetizing field where D is the demagnetizing factor and $= {}^2D/2\mu_0$. The coefficient *D* can be assumed to be constant since D is not a strong function of x [Dunlop, 1983b; Merrill, 1981 is in error]. The third term represents the interaction between the wall and a periodic array of pinning centers as a sinusoidal variation with wavelength λ. The temperature dependence of each term is contained in the reduced magnetization m.

Schmidt determines the possible stable wall positions by taking the derivative of (3.2.1-1) with respect to x and setting the result equal to zero. He shows that the extreme value for a stable wall position occurs at

$$S = \frac{\pi\ m^{p-2}}{\lambda} + \frac{H}{2\ \ m}, \qquad (3.2.1\text{-}2)$$

and that the blocking temperature occurs when S is a minimum, yielding

$$m_b \equiv m(T_b) \equiv \frac{M(T_b)}{M(0)} = \left(\frac{\lambda H}{2(p-2)\pi}\right)^{\frac{1}{p-1}}. \qquad (3.2.1\text{-}3)$$

As in the SD case, the blocking temperature is found to be a function of the applied field. At the blocking temperature the wall is pinned at or near $x_b = S_{min}$ where

$$M_b = \frac{^2H}{2\mu_0}\left(\frac{p-1}{p-2}\right) = \left(\frac{p-1}{p-2}\right)\frac{H}{D}. \qquad (3.2.1\text{-}4)$$

With further cooling,

$$M(T) = M(T_b)\frac{M_s(T)}{M_s(T_b)} = M_b\frac{m(T)}{m(T_b)}. \qquad (3.2.1\text{-}5)$$

The resulting TRM obtained by Schmidt is

$$M_{TRM} = m(T)\frac{^2(p-1)}{2\mu_0\ (p-2)}\left(\frac{2(p-2)\pi}{\lambda}\right)^{\frac{1}{p-1}} H^{\frac{p-2}{p-1}}. \qquad (3.2.1\text{-}6)$$

The coercive force is obtained by setting (3.2.1-2) equal to zero, giving

$$H_c(T) = \frac{2\pi\ m^{p-1}(T)}{\lambda}\ . \qquad (3.2.1\text{-}7)$$

This matches Néel's assumed variation of H_c with M_s if $p = 3$. Other workers have obtained values of p ranging from 2 to 10. The TRM can be written in terms of the coercive force as follows:

$$M_{TRM} = \frac{^2(p-1)}{2\mu_0\ (p-2)}((p-2)H_c)^{\frac{1}{p-1}} H^{\frac{p-2}{p-1}}. \qquad (3.2.1\text{-}8)$$

These arguments hold provided the maximum stable wall position given by (3.2.1-2) does not decrease when we remove the field at room temperature; otherwise, the wall will move to the maximum stable room-temperature position. The limiting case occurs for the applied field H_2 determined by setting $S(T_a, H = 0) = S(T_b, H_2)$, using (3.2.1-2) and (3.2.1-3), and solving for H_2. Saturation will occur if the applied field $H > H_2$, where

$$H_2 = \frac{2\pi}{\lambda}\left(\frac{p-2}{p-1}\right)\left(\frac{1}{p-1}\right)^{\frac{1}{p-2}} m^{p-1}(T_a) = \left(\frac{p-2}{p-1}\right)\left(\frac{1}{p-1}\right)^{\frac{1}{p-2}} H_c(T_a). \qquad (3.2.1\text{-}9)$$

The magnetization saturates at

$$M_s(T) = \frac{\pi}{\lambda\mu_0} m^{p-1}(T) = \frac{^2H_C}{2\mu_0} = \frac{H_C}{D}. \qquad (3.2.1\text{-}10)$$

Schmidt argues that thermal activation blocking will dominate in the low-field region where

$$H < H_1 = \frac{2\pi\ (p-2)}{\lambda}\left(\frac{p-1}{p-2}\right) m_{THB}\left(\frac{1}{p}\right)^{p-1} = (p-2)\left(\frac{p-1}{p-2}\right)\left(\frac{1}{p}\right)^{p-1} H_c(T_{THB}) \qquad (3.2.1\text{-}11)$$

where m_{THB} must be determined numerically from

$$m_{THB}(T_{THB}) = \left(\frac{kT_{THB}\ln(C'\tau_b)}{2\ v}\right)^{\frac{1}{p}} \qquad (3.2.1\text{-}12)$$

where C´ is a constant that is analogous to C in (3.1.1-2) (see Appendix E). Since m_{THB} is independent of H in the low field limit, so is T_{THB}, and by (3.2.1-4) and (3.2.1-5)

$$M_{THB}(T) = \frac{^2H}{2\mu_0}\left(\frac{p-1}{p-2}\right)\left(\frac{1}{m(T_{THB})}\right) = \left(\frac{p-1}{p-2}\right)\left(\frac{m(T)}{m(T_{THB})}\right)\left(\frac{H}{D}\right). \qquad (3.2.1\text{-}13)$$

This model has the following characteristics:

1. TRM is a continuous, monotonic, increasing function of the applied field.

2. TRM is a linear function of the applied field at low fields (3.2.1-13), proportional to $H^{\frac{p-2}{p-1}}$ for intermediate fields (3.2.1-6), and saturates at high fields (3.2.1-10). If Néel's suggestion of $p = 3$ is taken, the intermediate-field TRM is proportional to $H^{1/2}$.

There are three distinct regions in this model, versus a smooth variation in the SD models. Assuming that this model is correct, these three regions should be observable. In practice, this is very difficult because variations in grain size and microscopic coercivity act to smooth the $M_{TRM}(H)$ curve. Even if the observations showed three regions with the predicted H^1, $H^{1/2}$, and H^0 dependencies, that alone could not be cited as supporting the model for the simple reason that any reasonable smooth, monotonic, increasing model showing H^1 dependence at low fields and H^0 dependence at high fields would be expected to show $H^{1/2}$ dependency at some intermediate field.

Schmidt [ca. 1976] studied a two wall, two coercivity model developed along the lines of the model just presented. The two wall, two coercivity model cannot be solved analytically, so computer simulations were used to examine its behavior. One of the more interesting results is the prediction of a low-field $H^{\approx 0.7}$ dependence for $M_{TRM}(H)$. This was obtained without resorting to thermal-agitation blocking. This result merits further investigation.

3.2.2 Unblocking in the Néel wall-motion mechanism

In Schmidt's [1973] model of thermoremanence, the location of the domain wall at the blocking temperature is given by

$$x_b = \frac{\pi\, m_b^{p-2}}{\lambda} + \frac{H}{2\, m_b}. \qquad (3.2.2\text{-}1)$$

For the unblocking condition, $H = 0$ and so the extreme location for the energy minimum is given by

$$S_{ub} = \frac{\pi\, m_{ub}^{p-2}}{\lambda}. \qquad (3.2.2\text{-}2)$$

Now if $S(T) \geq x_b$ then unblocking does not occur, whereas if $S(T) < x_b$ it does. Setting $S(T) = x_b$ gives

$$\frac{\pi\, m_{ub}^{p-2}}{\lambda} = \frac{\pi\, m_b^{p-2}}{\lambda} + \frac{H}{2\, m_b}. \qquad (3.2.2\text{-}3)$$

Immediately we see that $m_{ub}(T) > m_b(T)$ for $H > 0$, and hence $T_{ub} < T_b$. The difference between T_{ub} and T_b widens as H increases, but slower than H since $\left(\frac{H}{m_b}\right)$ is controlling. We can rearrange the preceding equation to give

$$m_{ub}^{p-2} = m_b^{p-2} + \frac{\lambda H}{2\pi\, m_b} = m_b^{p-2} + (p-2)m_b^{p-2}, \qquad (3.2.2\text{-}4)$$

or

$$m_{ub} = (p-1)^{\frac{1}{p-2}}\, m_b. \qquad (3.2.2\text{-}5)$$

The leading coefficient ranges from 1 for $p \to \infty$ to $e = 2.718\ldots$ for $p \to 2^+$.

Thermal activation blocking replaces Néel blocking when $x_{th} < S_{min}$. It will be unblocked in zero field only when $x_{th} = S_{H=0}$. So

$$\frac{\pi\, m_{ub}^{p-2}}{\lambda} = \frac{H}{2\, m_{THB}}, \qquad (3.2.2\text{-}6)$$

or

$$m_{ub}^{p-2} = \frac{\lambda H}{2\pi\, m_{THB}} = \frac{(p-2)}{H_1}\left(\frac{p-1}{p-2}\, m_{THB}\right)^{p-1} \frac{H}{m_{THB}} = \frac{H}{H_1}(p-2)\left(\frac{p-1}{p-2}\right)^{p-1} m_{THB}^{p-2}, \qquad (3.2.2\text{-}7)$$

where H_1 is the highest field at which thermal activation blocking takes place (see 3.2.1-11). So

$$\frac{m_{ub}}{m_{THB}} = (p-2)^{\frac{1}{p-2}}\left(\frac{p-1}{p-2}\right)^{\frac{p-1}{p-2}}\left(\frac{H}{H_1}\right)^{\frac{1}{p-2}} = \left(\frac{H}{H_1}\right)^{\frac{1}{p-2}}, \qquad (3.2.2\text{-}8)$$

where *F* defined in this equation ranges from ∞ to 1 as p ranges from 2 to ∞, and has typical values of 4 to 10. If we define $H = H_3$ as the field at which

unblocking occurs at the same temperature as thermal activation blocking ($m_{ub} = m_{THB}$), we can solve for H_3 to obtain

$$H_3 = \frac{2\pi\, m_{THB}^{p-1}}{\lambda} = H_{C_{THB}}. \qquad (3.2.2\text{-}9)$$

Now H_3 is just H_C due to Néel blocking at $T = T_{THB}$. If H is less than this coercive force, then Néel unblocking is not possible and thermal activation unblocking takes over. So for $H < H_3$ we have $m_{ub} = m_{THB}$ and hence $T_{ub} = T_{THB}$. So for all H, $T_{ub} \le T_b$.

To summarize, $T_b - T_{ub}$ is zero for $H < H_3$, increases smoothly with increasing H until $H = H_1$, at H_1 it decreases substantially as H is increased through H_1, and then it increases with H above H_1.

3.2.3 Other MD theories

There are several other MD models; however, examination shows that they are merely variations of the same model. Schmidt's [1972] formulation was presented in Section 3.2.1 because it provides the clearest explanation in terms of fundamental, easily understood concepts. Schmidt's model starts with an energy expression, whereas Néel [1955] began by assuming the following expression for the coercive force:

$$\frac{H_c(T)}{H_c(0)} = \left(\frac{M_s(T)}{M_s(0)}\right)^2. \qquad (3.2.3\text{-}1)$$

Schmidt notes that his model is physically equivalent to Néel's [1955] model if $p = 3$. Dunlop and Waddington [1975] follow Néel, but generalize the coercive force relation to

$$\frac{H_c(T)}{H_c(0)} = \left(\frac{M_s(T)}{M_s(0)}\right)^n. \qquad (3.2.3\text{-}2)$$

This is equivalent to Schmidt's model with $p = n + 1$. Stacey [1958] proposed a model based on setting the internal field of the grain equal to zero. Dunlop and Waddington showed that this is equivalent to their model, and hence Schmidt's, when $p \rightarrow \infty$. Everitt [1962] proposed a model based on the relations

$$\frac{H_c(T)}{H_c(0)} = \left(\frac{T_c - T}{T_c}\right)^l \tag{3.2.3-3}$$

and

$$\frac{M_s(T)}{M_s(0)} = \left(\frac{T_c - T}{T_c}\right)^m \tag{3.2.3-4}$$

and also allowed the applied field H to make an angle α with the domain wall. The predictions of Everitt's model are equivalent to Schmidt's in the high field limit if $p = \frac{l+m}{m}$. Everitt derived the following expression for the TRM:

$$M_{TRM} = \frac{\mu_0 H \sin\alpha}{N}\left(\frac{H_c(0)}{aT_b}\right)^{\frac{m}{l+m}}\left(1 - \frac{m}{l+m}\left(\frac{H\sin\alpha}{H_c(0)}\right)\left(\frac{H_c(0)}{aT_b}\right)^{\frac{l}{l+m}}\right) \tag{3.2.3-5}$$

where

$$a = \frac{k \ln\left(\frac{\tau_b}{\tau_0}\right)}{cS\lambda\mu_0 M_s(0)}, \tag{3.2.3-6}$$

S is the area of the wall, λ is the width of the energy barrier that the wall must pass, and c is a factor determined by the shape of the barrier. Although this model brings in some geometric refinements that are not incorporated in Schmidt's model, the physical processes involved are the same.

Day [1977] provides a nice summary of each of these models.

The kinematic model of McClelland and Sugiura [1987], expanding on the model of Sugiura [1981], should be mentioned in passing. Their model is based on the assumption that when a rock is cooled in a magnetic field through the Curie temperature, the magnetization at any temperature is in a state equivalent to the total TRM, except the spontaneous magnetization is smaller at higher temperature. This can be written as follows:

$$PTRM_{T}^{T_c}(T) = TRM(T)\frac{M_s(T)}{M_s(0)} \qquad (3.2.3\text{-}7)$$

Note that there is no field dependence in this model other than the field dependence of the TRM. This model is unique in that it gives the PTRM spectrum without explicitly assuming a grain size or microscopic coercivity spectrum. This model was developed to explain TRM properties observed in large (≈200 μm) magnetite grains, and does not appear to apply to the 1 to 2 μm grains studied here.

3.3 PSD theories

The transition between SD and MD particles is expected to occur at a particle size where the reduction in magnetostatic energy achieved by taking on a domain structure offsets the increase in exchange energy associated with a domain wall. Calculated sizes for the transition depend somewhat on the assumptions made. Day [1977] summarized the work of several authors, showing that most estimates place the transition at about 0.03 to 0.1 μm for equidimensional magnetite grains. The critical size increases as the length to width ratio of the particle increases.

Multidomain particles are expected to have low coercivities and low remanence; however, this is not observed for small MD grains. The discontinuities in various magnetic properties (e.g., H_c, $\frac{H_c}{H_c^{max}}$, $\frac{M_{rs}}{M_s}$) have not been observed (see Dunlop [1981]). Instead, there appears to be a gradual transition between the magnetic properties at the SD to MD transition size and the properties predicted by MD theory, which become dominant at about

20 μm. Stacey [1962] postulated the existence of pseudo-single domain moments in small MD particles, with properties approaching those of true SD particles. Since then, several candidates have been suggested for the origin of these moments. The following sections describe the principal candidates.

3.3.1 Barkhausen discreteness of domain wall movements

Stacey [1962] introduced the concept of pseudo-single-domain moments, and explained them in terms of the Barkhausen discreteness in the position of the domain walls. He obtained the following expression for the spontaneous grain moment:

$$= \frac{9}{16}\frac{r d_0^3 M_s}{1+D\chi}\left(\frac{d}{d_0}\right)^{\frac{3}{2}} \tanh\left(\frac{1}{2\sqrt{3}}\frac{d}{d_0}\right) \qquad (3.3.1\text{-}1)$$

where d_0 is the critical minimum SD size, χ is the intrinsic low-field susceptibility, and r is the net number of incremental moments in one direction. By assuming that the net alignment of the spontaneous moments of an assembly of grains in a field H is given by Boltzmann's distribution, and that blocking occurs as in Néel's [1955] SD theory, Stacey obtains

$$M_{TRM} = \bar{\alpha}\, n_v \tanh\left(\frac{\bar{\alpha}\mu_0\, m_b(T_b)H}{kT_b}\right) \qquad (3.3.1\text{-}2)$$

where $\bar{\alpha} \approx 0.85$ is the mean direction cosine between domain directions and the applied field. This gives essentially the same $T_b(H)$ dependence as in the single domain model (see equation 3.1.1-8). Stacey concludes that "there is nothing fundamental about the transition from PSD to MD behavior, since the grain size at which it occurs is a function of the applied field," (see figure 1). This fact appears to have been overlooked by later workers.

Dunlop [1977] argues that Barkhausen discreteness cannot account for PSD behavior because the moments cannot reverse independently from the

domain moments. In addition, he felt that the interaction between the moments in larger grains would minimize their resultant moment.

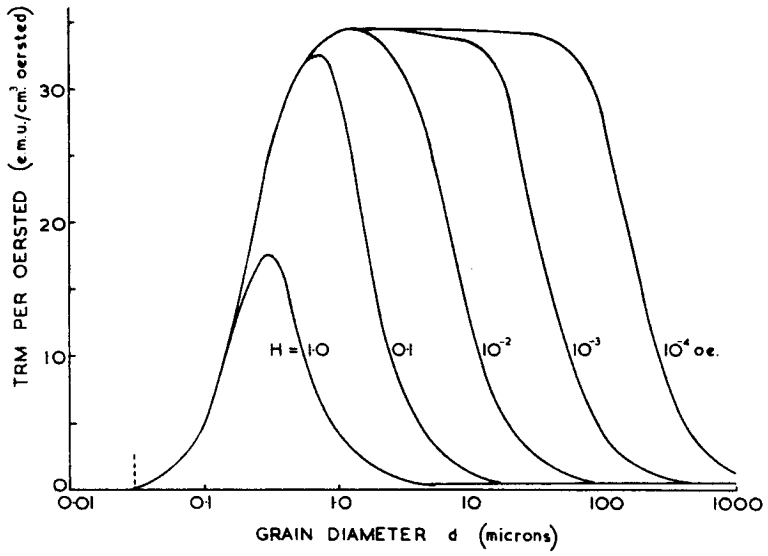

Figure 1 TRM versus grain size and applied field in Stacey's [1962] model of PSD behavior.

3.3.2 Surface domains

Stacey and Banerjee [1974], Banerjee [1977], and Moskowitz and Banerjee [1979] appeal to surface moments controlled by local surface anisotropy. This model immediately gives a $M_{TRM} \propto d^{-1}$ dependence. Day [1977] collected the available data and obtained $M_{TRM} \propto d^{-0.7}$, which is consistent within the limits of the available data.

Stacey and Banerjee assume that the PSD moments are random effects arising from imperfections in surface domain structures. They arbitrarily assume that there are $n (\propto d^{-1})$ such moments per unit volume, with magnitudes that are uniformly distributed between 0 and σ_{psd}^{max}. By assuming a constant blocking temperature, they obtain the following expression for the TRM:

$$M_{TRM} = n\,\sigma_{psd}^{max}\int_0^1 dy\int_0^1 xy\,\tanh\left(\frac{\sigma_{psd}^{max}H}{kT_b}\frac{M_s(T_b)}{M_s(0)}xy\right)dx \equiv n\,\sigma_{psd}^{max} f(\alpha H) \qquad (3.3.2\text{-}1)$$

This is superimposed on the TRM obtained by MD theory. Dunlop, et al [1974] compared the TRM acquired by magnetite particles in the 0.04 μm to 0.22 μm range to an equation of the form

$$M_{TRM} = aH + bf(\alpha H) \qquad (3.3.2\text{-}2)$$

where the linear term is typical of low-field MD theories. They obtained good agreement for $300\ \mu T \le H \le 2\ mT$. Systematic deviations in higher fields were qualitatively attributed to the known nonlinearity of MD TRM on H, and the field dependence of T_b. Deviations observed for lower fields were not explained.

3.3.3.Domain wall moments

Dunlop [1977] argued that only the net moments of domain walls could qualify as subdomain moments with true SD-like behavior. He argues that equation (3.1.1-2) can be applied to these moments, which he called “psarks.”

Dunlop found evidence for psarks in 0.05 to 0.26 μm magnetite grains by isolating part of the initial susceptibility and weak-field TRM that is not controlled by the internal demagnetizing field, and by determining the volume activated in TRM and high-temperature IRM and comparing it to the volume of a domain wall. There has been less success with larger grains. Dunlop and Bina [1977] analyzed the high-temperature hysteresis and alternating field demagnetization of 1.0 to 5.0 μm magnetite grains. No evidence for psarks was found, despite the fact that PSD moments appear to exist in this size range. Dunlop [1977] concludes that the PSD moments are “either coupled to the main domains (i.e., not SD-like) or, if independent, too large to respond noticeably to thermal agitation.” He concludes that psarks cannot explain the PSD behavior observed in magnetite grains larger than 1.0 μm.

3.3.4 Moments pinned by dislocation stress fields

Verhoogen [1959] felt that the stress fields introduced by dislocations in the crystal structure were the only mechanism likely to result in coercive forces in excess of about 300 kA m^{-1} for MD magnetite. Ozima and Ozima [1965] felt that small regions isolated from the surrounding matrix by submicroscopic grain boundaries of at least several tens of interatomic distances were a more likely cause. Kobayashi and Fuller [1968] assumed that the moments associated with stress centers had a higher blocking temperature than the remainder of the grain, and obtained the following expression:

$$_{TRM} = \frac{nv_0 M_s(T_a)}{3(1+D\chi_m)} \tanh\left(\frac{v_b \mu_0 M_s(T_b) H}{kT_b}\right), \qquad (3.3.4\text{-}1)$$

where n and v_b are the number and volume of in-phase stress centers at T_b, v_0 is the volume of the individual pinned domains at temperature $T_0 << T_b$, and χ_m is the susceptibility of the matrix at the temperature at which the volume of the pinned regions reaches the final value v_0 . This gives essentially the same $T_b(H)$ dependence as in the single domain model (see equation 3.1.1-8).

Dickson, et al [1966] argued that Verhoogen's model could not apply to magnetite because the magnetostatic energy of a SD region would completely dominate the magnetocrystalline anisotropy and magnetostatic strain energies, making it impossible for such a region to behave independent of the matrix. Dunlop [1977] pointed out that the moments associated with stress-pinning of spins can only be reversed when traversed by a 180° domain wall, and hence could not be the source of independent SD-like behavior.

3.3.5 Metastable SD-like states

Halgedahl and others (e.g., Halgedahl and Fuller [1980, 1983]; Boyd, Fuller and Halgedahl [1984]) monitored the magnetic domain patterns for various titanomagnetite grains under varying fields, and concluded that the difficulty of nucleating domain walls can explain several aspects of PSD behavior. They identified two processes by which domain walls can be nucleated: creation of walls at surface imperfections, and unpinning of minute wall fragments from strong potential energy traps at the grain surface.

There seems to be little doubt that the difficulty of nucleating domain walls has important implications for explaining PSD behavior; however, no quantitative models have been proposed that can predict the observed TRM behavior of PSD grains.

3.3.6 Intrinsic SD-like properties of small MD grains

Fuller [1984] argued that PSD behavior was in part due to an intrinsic grain size dependence of $\frac{J_R}{J_S}$, in addition to the variation in $\frac{J_R}{J_S}$ caused by the

difficulty in nucleating domain walls. His model was primarily based on attempts to fit empirical data, rather than derivations from first principles. This model was not developed to the point where it could be used to make significant predictions about TRM behavior.

3.4 Micromagnetic models

An entirely different approach is to perform calculations at the micromagnetic level where spin arrangements, not domain arrangements, are calculated. Domain patterns appear automatically when the spin configurations that minimize the total grain energy are determined. The energy minima found may be either global or local, with the latter being necessary to account for the thermal behavior of TRM.

The ideas of the micromagnetic approach are quite old, having first appeared in Landau and Lifshitz's [1935] article on domain theory. Early analytical calculations include those of Bitter [1937], Elmore [1938], and Brown [1940, 1959], but the complexity of the calculations limited progress until recent advances in computer technology made the problem more tractable. Recent studies examined both the one-dimensional (e.g., Moon and Merrill [1984, 1985], Moon [1985]) and three-dimensional (e.g., Schabes and Bertran [1988], Williams and Dunlop [1988, 1989, 1990], Shcherbakov et al [1990]) cases. Surprisingly, the typical octahedral form for magnetite has not yet been modeled, nor have most micromagnetic models considered the fact that, in magnetite, [111] are the easy directions and [100] are the hard directions.

The micromagnetic approach can give insight on the detailed magnetic structure of a perfect crystal, but is less suited to modeling assemblages of imperfect grains. The method suffers from its inability to express any final results in an analytical form, and the corresponding need for tremendous computer resources to predict quantitative trends.